Chapter 2. Identifying the Presence of a Disulfide Linkage in Peptides by the Selective Elimination of Hydrogen Disulfide from Collisionally Activated Alkali and Alkaline Earth Metal Complexes

2.1. Abstract

We report a new method for identifying disulfide linkages in peptides using mass spectrometry. This is accomplished by collisional activation of singly charged cationic alkali and alkaline earth metal complexes, which results in the highly selective elimination of hydrogen disulfide (H_2S_2). Complexes of peptides possessing disulfide bonds with sodium and alkaline earth metal are generated using electrospray ionization (ESI). Isolation followed by collision induced dissociation (CID) of singly charged peptide complexes results in selective elimination of H_2S_2 to leave newly formed dehydroalanine residues in the peptide. Further activation of the product yields sequence information in the region previously short circuited by the disulfide bond. For example, singly charged magnesium and calcium ion bound complexes of [Lys^8]-vasopressin exhibit selective elimination of H_2S_2 via low energy CID. Further isolation of the product followed by CID yields major b- and z-type fragments revealing the peptide sequence in the region between the newly formed dehydroalanine residues. Numerous model peptides provide mechanistic details for the selective elimination of H_2S_2. The process is initiated

starting with a metal stabilized enolate anion at Cys, followed by cleavage of the S-C bond. An examination of the peptic digest of insulin provides an example of the application of the selective elimination of H_2S_2 for the identification of peptides with disulfide linkages. The energetics and mechanisms of H_2S_2 elimination from model compounds are investigated using density functional theory (DFT) calculations.

2.2. Introduction

The formation of disulfide bonds by linking cysteine residues (Cys) is an important post-translational modification (PTM) process, which is critical for the three-dimensional structures of proteins and their stabilities.[1-3] Determination of disulfide bonds is an essential part of protein analysis for the comprehensive understanding of protein structures.[2] The development of practical applications of mass spectrometry for the identification of disulfide bonds in peptides remains an active and challenging field of research. Tandem mass spectrometry (MS^n) has been widely used for the identification of various PTM sites in peptides.[4-11] However, disulfide bonds in peptide ions are not readily revealed by MS^n because of myriad low energy fragmentation pathways available to protonated peptides. Cleavage of disulfide bonds is not generally observed under low energy CID conditions.[2] A recent study reported that the energy required for cleavage at the disulfide linkage (S-C or S-S bonds) is ~40–70 kcal/mol in protonated cystine and its derivatives, while cleavage at the amide bond requires typically ~25-40 kcal/mol.[12] The presence of disulfide bonds often inhibits cleavage of short intervening cyclic regions of the peptide ion.[13] This makes it difficult to obtain sequence information in regions of the peptide short circuited by disulfide bonds.

A number of studies have reported selective cleavage of the S-S or S-C bond at disulfide linkages in peptide cations[12,14] and anions[15-17] using low energy CID and in the absence of a mobile proton. However, the fragments formed in competitive cleavages involving S-C and S-S bonds in peptide cations can lead to complex and difficult to interpret MS^n spectra. Of particular interest in relation to the present study, Bowie and co-workers have reported elimination of hydrogen disulfide (H_2S_2) under low energy CID conditions from anionic peptides with disulfide bonds.[15] They proposed a mechanism where H_2S_2 elimination is initiated via Cys backbone enolation.[15] These characteristic dissociation pathways of an anionic peptide allow identification of the existence of disulfide bonds in the peptide. Further, MS^3 of the product peptide anion yields cleavage products that provide more complete structural analysis of the peptide.[15,18] However, this application is limited mainly to acidic peptides, which readily deprotonate to form anions using ESI.[15,18] Both S-S and S-C bond cleavages at disulfide linkages occur under electron capture dissocation (ECD) conditions.[19,20] These processes occur in competition with the extensive backbone cleavage reactions observed with ECD.

A wide range of investigations of the interactions of metal cations with peptides in the gas phase have been reported.[21-25] In numerous instances metal cations have been shown to play a unique role in stabilizing specific peptide structures in the gas phase, exemplified by the formation of stable helical peptides.[22] Other reports demonstrate that collisional activation of metal peptide complexes can provide unique sequence information.[26-34] Of particular interest are several studies reporting applications of metal ions to the selective dissociation of peptides with disulfide bridges.[20,26,32,35] Transition metal (Ni^{2+}, Co^{2+}, and Zn^{2+}) complexes of oxytocin exhibit dissociation pathways related to S-S and S-C bond cleavages under ECD conditions.[20] A recent fourier transform mass

spectrometry (FTMS) study reported that sustained off-resonance irradiation collision induced dissociation (SORI-CID) of the transition metal (Ni^{2+}, Co^{2+}, and Zn^{2+}) complexes of oxytocin and analogs readily yield products involving S-S and S-C bond cleavages.[26] McLuckey and co-workers have reported selective S-S bond cleavage in cationic gold(I) complexes of peptides under low energy CID conditions.[32]

A widely used methodology for identify disulfide linkages in proteins, normally not employing MS^n methods, involves the MS analysis of disulfide linked peptides generated from pepsin digests.[2] This is usually compared to the MS of the same digest in which the disulfide linkages are cleaved. However, pepsin produces complex digests, making it difficult to interpret the MS data. In a novel approach, Gorman and co-workers have examined the incorporation of the ^{18}O isotope into peptides during peptic digestion of disulfide-linked proteins in 50% $H_2{}^{18}O$.[36] Using this approach they have characterized disulfide linkages in the proteins from the isotope patterns and increases in average masses of the digest products.

In the present paper, we report highly selective elimination of H_2S_2 from sodiated and alkaline earth metal bound peptide cations with disulfide linkages under low energy CID conditions. The structures of compounds examined in this study are shown in Figure 1. Preference for selective dissociation processes involving the disulfide bridge is investigated under low energy CID conditions using a series of singly charged sodiated cystine cations with various number of sodium cations. The model peptides AARAAACAA (MP1) and the disulfide bridge linked dimer $(AARAAACAA)_2$ (MP2) are investigated as cationic complexes with sodium and several alkaline earth metals. Singly charged cationic metal complexes of MP1 and MP2 exhibit highly selective elimination of H_2S and H_2S_2, respectively, via CID. To test the generality of the latter

Figure 1. Structures of cystine, model peptides, nonapeptide hormones, and insulin examined in this study.

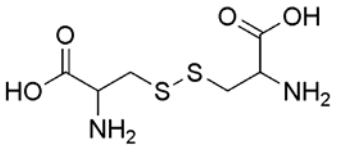

Cystine

Ala-Ala-Arg-Ala-Ala-Ala-Cys-Ala-Ala

Model Peptide 1 (MP1)

Ala-Ala-Arg-Ala-Ala-Ala-Cys-Ala-Ala
Ala-Ala-Arg-Ala-Ala-Ala-Cys-Ala-Ala

Model Peptide 2 (MP2)

Cys-Tyr-Phe-Gln-Asn-Cys-Pro-Lys-Gly-NH_2

[Lys^8]-vasopressin (LVP)

Cys-Tyr-Ile-Gln-Asn-Cys-Pro-Leu-Gly-NH_2

Oxytocin (OT)

A chain
Gly-Ile-Val-Glu-Gln-Cys-Cys-Ala-Ser-Val-Cys-Ser-Leu-Tyr-Gln-Leu-Glu-Asn-Tyr-Cys-Asn

B chain
Phe-Val-Asn-Gln-His-Leu-Cys-Gly-Ser-His-Leu-Val-Glu-Ala-Leu-Tyr-Leu-Val-Cys-Gly-Glu-Arg
Ala-Lys-Pro-Thr-Tyr-Phe-Phe-Gly

Insulin

process and its utility as a method for locating disulfide linkages in peptides, we have examined the nonapeptide hormones [Lys^8]-vasopressin (LVP, CYFQNCPKG-NH_2) and oxytocin (OT, CTIQNCPLG-NH_2). These nonapeptide hormones, which contain an intramolecular disulfide bond, have been widely used for the investigation of the interactions of peptides with metal cations in gas phase[24,37,38] and for the identification of disulfide bonds.[20,26] Again, highly selective elimination of H_2S_2 is observed, and further MS^n spectra reveal additional details of the peptide structure. Further application of this technique for the identification of peptides with a disulfide linkage is demonstrated by examining the peptic digest of insulin. The mechanisms and energetics of the observed reactions are evaluated by means of computational modeling.

2.3. Experimental

L-cystine hydrochloride solution, calcium dichloride ($CaCl_2$), insulin from bovine pancreas, iodine (I_2), magnesium dichloride ($MgCl_2$), pepsin from porcine stomach mucosa, and sodium chloride (NaCl) were purchased from Sigma-Aldrich (St. Louis, MO). The model peptide AARAAACAA was purchased from BiomerTechnology (Concord, CA). The nonapeptide hormones OT and LVP were purchased from GenScript (Piscataway, NJ). All solvents (water and methanol) are HPLC grade and were purchased from EMD Chemicals Inc. (Gibbstown, NJ). For the formation of an intermolecular disulfide bond joining pairs of MP1, 10 mM of the peptide was dissolved in a 50:50 methanol/water mixture containing 10 mM of I_2. The solution was stirred vigorously for 15 minutes and left 2 hours at room temperature. The dimeric peptide product MP2 linked via a disulfide bond was confirmed by the ESI mass spectrum. All metal complex samples were prepared by dissolving stoichiometric amounts of metal chloride and the

analyte sample in the solvent. The total concentration of the sample solution was fixed as 100 μM. Pepsin digests of insulin were prepared by incubating 0.1 mg of insulin from bovine pancreas with 0.025 mg of pepsin from porcine stomach mucosa in water containing 1% acetic acid by volume at 37 °C for 6 hours. Then pepsin was filtered out using a Millipore Microcon centrifugal filter fitted with an Ultracel YM-10 membrane. The sample solution was diluted to an appropriate concentration for ESI. A sodiated sample was prepared by dissolving 40 μM of sodium chloride in the diluted peptic digest solution.

Experiments were performed on a Thermo Finnigan LCQ Deca ion trap mass spectrometer (ITMS) in positive mode. Electrospray voltage of 5 kV, capillary voltage of 9 V, and capillary temperature 275 °C were set as parameters for ESI. The temperature of the MS analyzer was ~23 °C before the experiment and ~24 °C during the experiment. The pressure is estimated to be ~10^{-3} torr He inside the trap. Metal complex ions of interest were isolated and fragmented via low energy CID. Continuous isolation of the cluster ions followed by CID (MS^n) was performed until the track of the isolated ion was lost. The ESI mass spectra reported in this study were obtained by averaging 30 scanned spectra.

The mechanisms and energetics of the observed reactions are evaluated based on optimized structures and their corresponding energies for reactants and products using density functional theory (DFT) calculations. More than 500 possible molecular conformations were investigated through dihedral angles from -180° to 180° and their corresponding potential energy maps were determined at the augmented PM5 level using CAChe 6.1.10 (Fujitsu, Beaverton, OR). Then, the lowest-energy structures were

determined using DFT with a number of candidate low energy structures from the PM5 calculations. The DFT calculations were performed using Jaguar 6.0 (Schrödinger, Portland, OR) utilizing the Becke three-parameter functional (B3)[39] combined with the correlation functional of Lee, Yang, and Parr (LYP).[40] For the disodiated cystine, the 6-31G** basis set[41] was used, then further DFT optimizations were carried out using the 6-311G** basis set. For the magnesium bound CGGCG and deprotonated CGGCG, the LACVP basis set was used. Thermodynamic properties were calculated assuming ideal gas at 298.15 K.

The nomenclature proposed by Roepstorff and Fohlman[42] was used for the parent and fragment ions. The prefixes "ds" and "Δ" refer to ions containing a disulfide bond and dehydroalanine, respectively. The numerical subscript refers to the number of units in the molecular ion when more than one repeated monomeric unit exists in a molecule. For example, an ion with two peptides, which are X and Y, linked via two disulfide bonds is referred as "ds_2XY." The dehydroalanine residue is referred to as "dA" in displayed peptide sequences.

2.4. Results

2.4.1. Sodiated Cystine Cation. The low energy CID spectra of singly charged protonated and sodiated cystine cations are shown in Figure 2. The proposed structures of the products and the dissociation mechanisms of the disodiated cystine are shown in Scheme 1. As seen in Figure 2a, CID of the protonated cystine cation yields major products resulting from the loss of [CO + H_2O] and two competitive products from S-C bond cleavages (-87 and -89 mass units). In addition, minor products resulting from loss of NH_3, H_2O, and NH_3 + [CO + H_2O] are observed in the spectrum. CID of the sodiated

Figure 2. CID spectra of (a) protonated cystine, (b) singly sodiated cystine, (c) doubly sodiated cystine, and (d) triply sodiated cystine cations. Arrows indicate the ion peaks being isolated and collisionally activated.

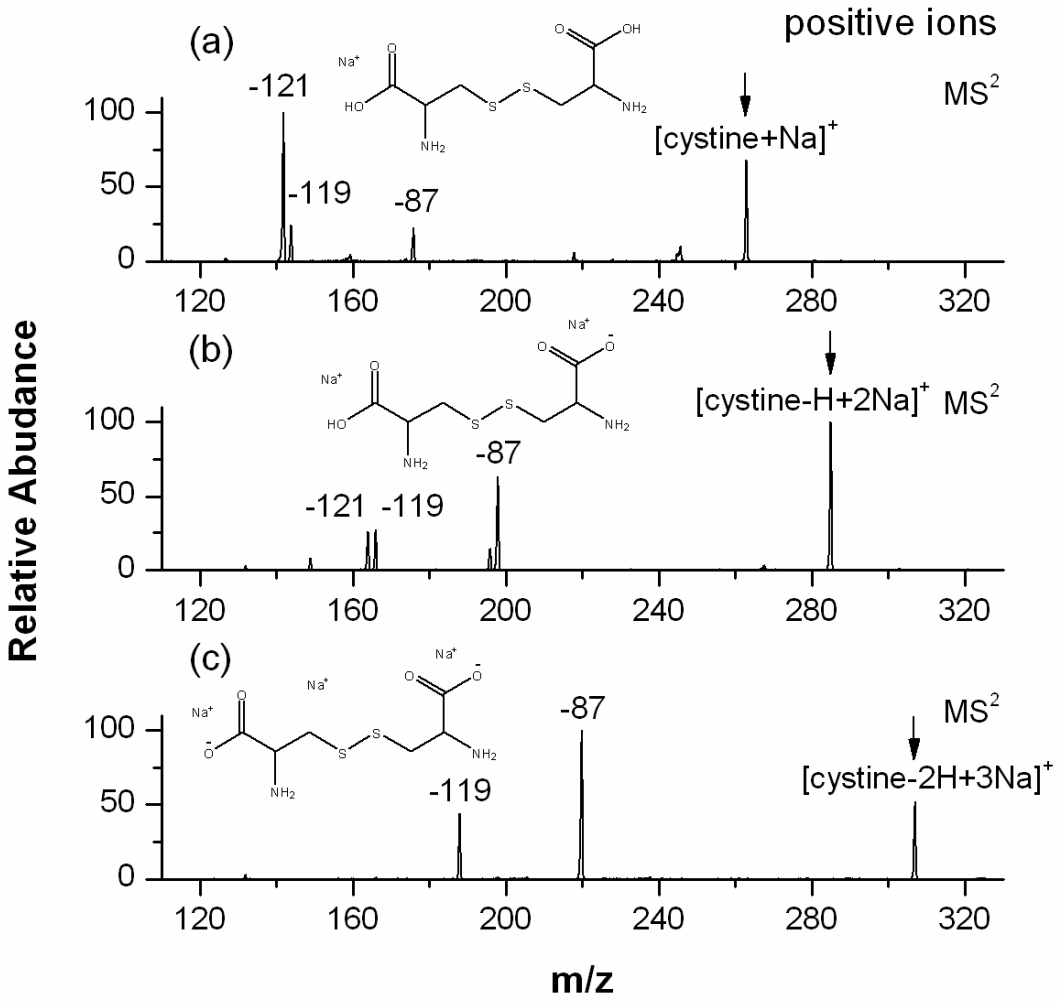
positive ions
(a)
-121
-119
-87
[cystine+Na]+
MS2
(b)
-87
-121 -119
[cystine-H+2Na]+
MS2
(c)
-87
-119
MS2
[cystine-2H+3Na]+
Relative Abudance
m/z
100
50
0
120
160
200
240
280
320

Scheme 1. Proposed dissociation mechanisms of disodiated cystine cation via CID. Optimized geometries and energy changes for corresponding numbered step are shown in Figure 10.

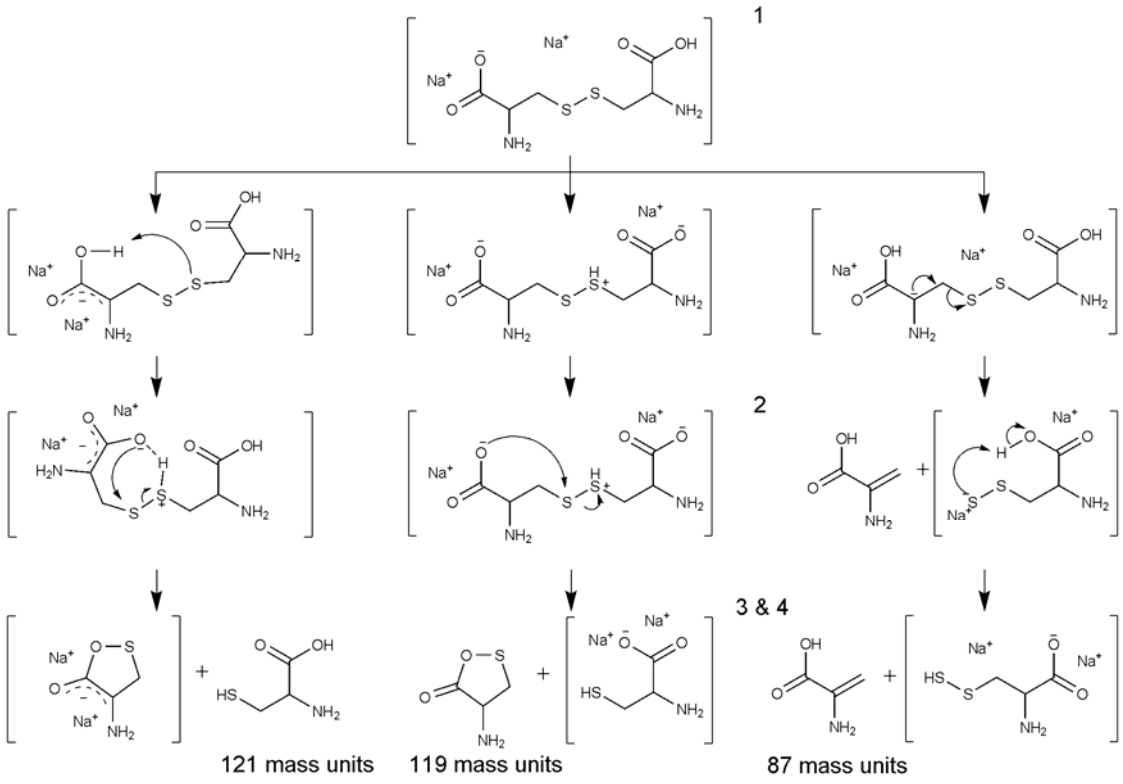

cystine cations yields products resulting from S-S bond cleavages (-119 and -121 mass units) and S-C bond cleavages (-87 and -89 mass units). In contrast to the protonated cystine cation, CID of the sodiated cystine cation exhibits significant cleavage of the S-S bond. The relative abundance of the CID products from S-S bond cleavage decreases as the number of sodium cations increase, while the product abundance from S-C bond cleavage increases (Figure 2b-d). The abundance of the product resulting from elimination of neutral cysteine (-121 mass units) decreases as the number of sodium cations increases in the complex. In contrast, the abundance of the product corresponding to loss of 119 mass units ($C_3H_5NO_2S$) increases as the number of sodium cations increases. The process involving loss of 119 mass units from CID of the trisodiated cystine cation yields the only product associated with S-S bond cleavage. The product resulting from the loss of 87 mass units (dehydroalanine) is observed as a dominant product from S-C bond cleavages in all three CID spectra of the sodiated cystine cations. In summary, CID of singly charged trisodiated cystine cation yields two distinct products, the loss of dehydroalanine (-87 mass units) and the loss of 119 mass units ($C_3H_5NO_2S$), that result from cleavage of the S-C and S-S bonds, respectively (Figure 2d and Scheme 1).

2.4.2. Metal Complexes of MP1. Figure 3 shows the low energy CID pathways of singly charged cationic complexes of MP1 with a proton, sodium cation, magnesium (Mg^{2+}) cation, and calcium cation (Ca^{2+}). The collisionally activated protonated model peptide dissociates to yield a broad range of b- and y-type fragments. Figure 3b and 3c show CID spectra of the sodiated peptide. As the number of sodium cations increases, selective elimination of H_2S from the side chain of the cysteine residue (Cys) is enhanced. The abundance of the product ion involving the loss of H_2S increases from 83% to 92%

Figure 3. CID spectra of singly charged (a) protonated AARAAACAA, (b) monosodiated AARAAACAA, (c) disodiated AARAAACAA, (d) monomagnesium AARAAACAA, and (e) monocalcium AARAAACAA. Arrows indicate the ion peaks being isolated and collisionally activated.

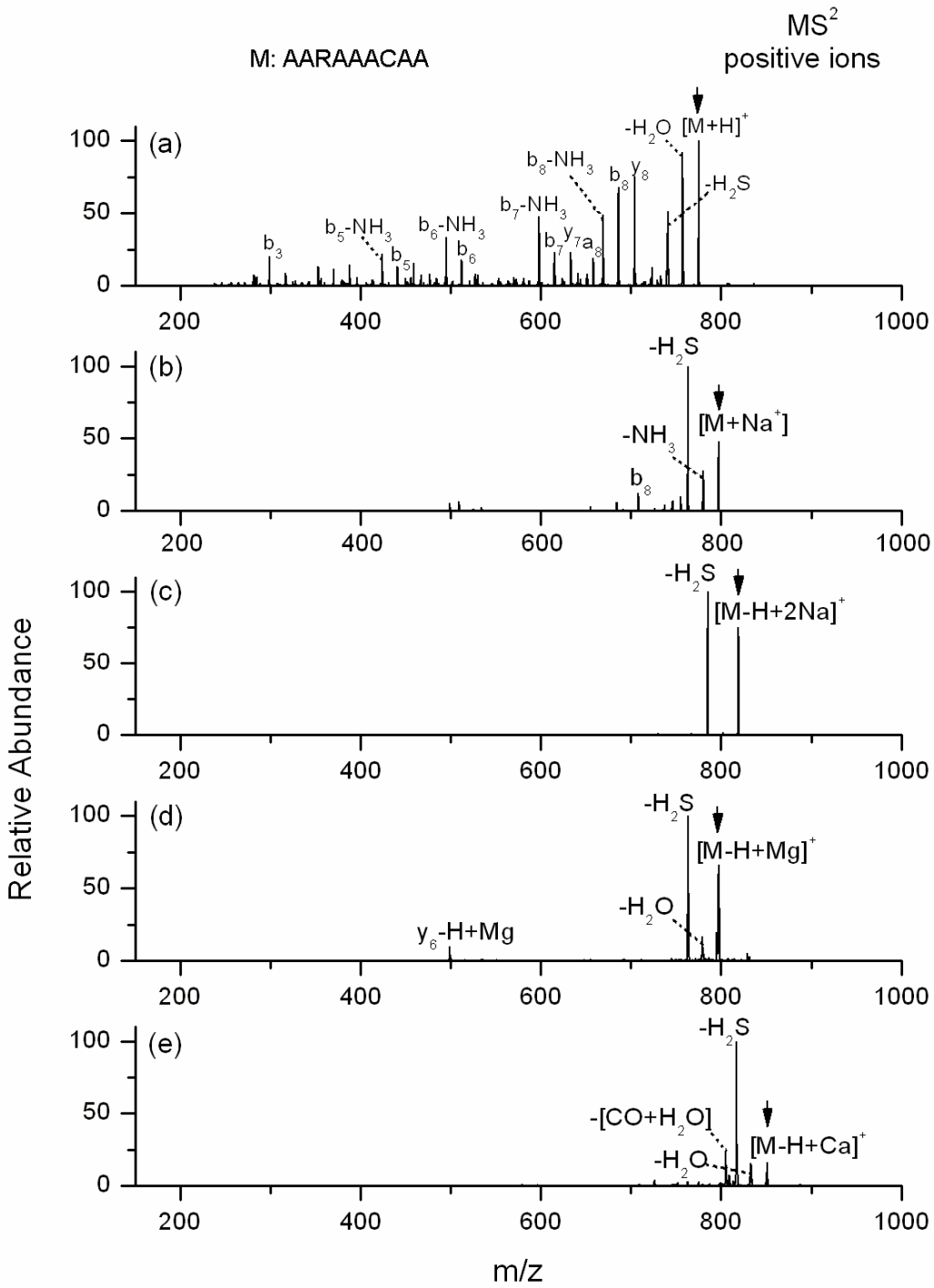
MS2
positive ions
M: AARAAACAA
(a)
(b)
(c)
(d)
(e)
Relative Abundance
m/z
[M+H]+
-H2O
-H2S
b8-NH3
b8
y8
b7-NH3
b5-NH3
b6-NH3
b3
b5
b6
b7
y7
a8
[M+Na+]
-NH3
[M-H+2Na]+
[M-H+Mg]+
y6-H+Mg
-[CO+H2O]
[M-H+Ca]+

of the total product ion intensity as the number of sodium cations increases from one to two in the complex. Alkaline earth metal (Mg^{2+} and Ca^{2+}) bound peptides also exhibit highly selective elimination of H_2S (Figure 3d and 3e).

2.4.3. Metal Complexes of MP2. Singly charged cationic sodium and divalent alkaline earth metal (Mg^{2+}, Ca^{2+}) complexes of MP2, which is the dimeric model peptide $(AARAAACAA)_2$ linked by a intermolecular disulfide bond, are examined. The low energy CID spectra of the singly protonated and singly sodiated peptides are shown in Figures 4a and 4b, respectively. The CID of the protonated and sodiated peptides yields four distinct products. A minor product resulting from the elimination of H_2S_2 is observed from the singly sodiated peptide. The products from S-C bond cleavage are observed at m/z 741.4 and m/z 807.3 from the protonated peptide and at m/z 763.5 and m/z 829.3 from the singly sodiated peptide. The products at m/z 741.4 in Figure 4a and at m/z 763.5 in Figure 4b contain the dehydroalanine (dA) residue from Cys. The products at m/z 807.3 and m/z 829.3 in Figures 4a and 4b, respectively, are the peptides with Cys converted to a disulfide. The products from S-S bond cleavages are shown at m/z 773.4 and m/z 775.3 from the protonated peptide and at m/z 795.3 and m/z 797.4 from the singly sodiated peptide. The products at m/z 773.4 in Figure 4a and at m/z 795.3 in Figure 4b comprise peptide fragments containing the thioaldehyde group (S=CHR). The products at m/z 775.3 in Figure 4a and at m/z 797.4 in Figure 4b are protonated and singly sodiated AARAAACAA peptide ions, respectively. Figure 4c shows the CID spectrum of the disodiated peptide. A dramatic increase of the relative abundance of the product from the elimination of H_2S_2 is observed compared to the protonated and singly sodiated peptides in Figures 4a and 4b. The products at m/z 785.3, m/z 817.4, and m/z 851.1 correspond to the disodiated AARAAAdAAA, AARAAACAA, and the

Figure 4. CID spectra of (a) protonated and (b) monosodiated intermolecular disulfide linked AARAAACAA dimer showing products from S-S and S-C bond cleavages. (c) CID spectrum of disodiated disulfide linked AARAAACAA dimer showing products from elimination of H_2S_2 and H_2S along with products from the disulfide bond cleavages. (d) CID spectrum of trisodiated disulfide linked AARAAACAA dimer showing major products from elimination of H_2S_2 and H_2S with some minor products from disulfide bond and backbone cleavages. (e) MS^3 spectrum of the product from elimination of H_2S_2 in (d). Arrows indicate the ion peaks being isolated and collisionally activated.

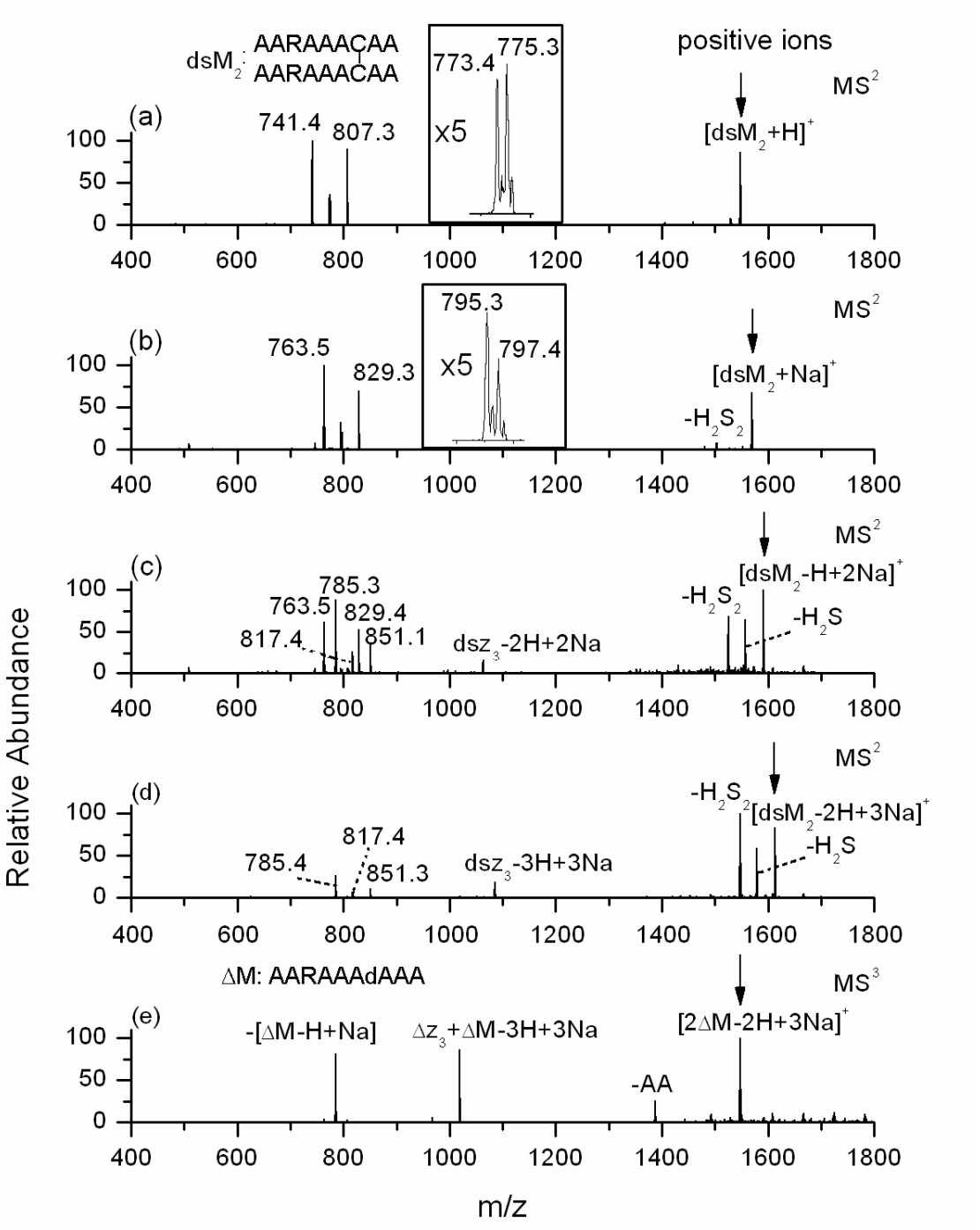
dsM2: AARAAACAA
AARAAACAA
positive ions
(a)
741.4
807.3
773.4
775.3
x5
MS2
[dsM2+H]+
(b)
763.5
829.3
795.3
797.4
x5
MS2
[dsM2+Na]+
-H2S2
(c)
785.3
763.5
829.4
817.4
851.1
dsz3-2H+2Na
MS2
[dsM2-H+2Na]+
-H2S2
-H2S
(d)
817.4
785.4
851.3
dsz3-3H+3Na
MS2
-H2S2
[dsM2-2H+3Na]+
-H2S
ΔM: AARAAAdAAA
MS3
(e)
-[ΔM-H+Na]
Δz3+ΔM-3H+3Na
-AA
[2ΔM-2H+3Na]+
Relative Abundance
m/z

Scheme 2. Dissociation pathways of singly charged trisodiated MP2 cation inferred from CID. Indicated product probed by MS^3. The locations of cleavages to form z_3 (b) and b_7 (c) fragments are shown in the lower part of the diagram.

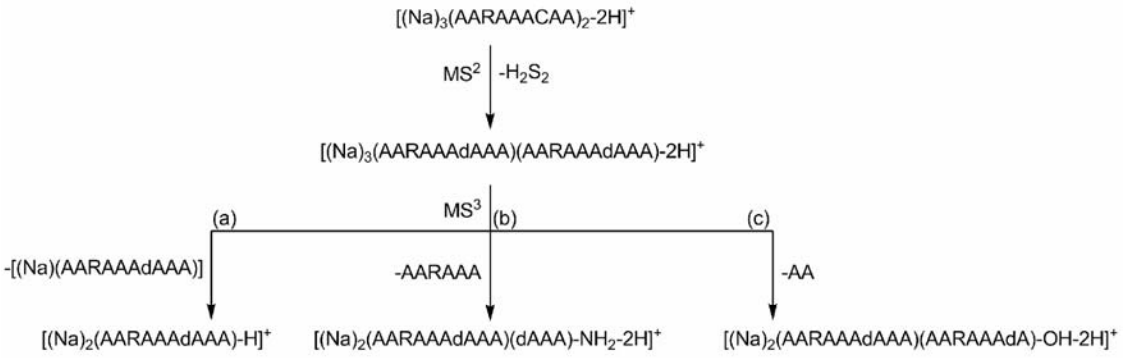

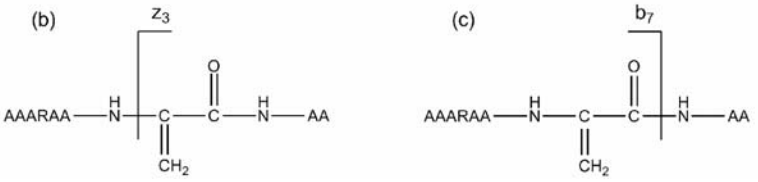

Figure 5. (a) MS^2 spectrum of singly charged monomagnesium complex of disulfide linked AARAAACAA dimer showing a major product from elimination of H_2S_2 and a minor product from H_2S elimination. (b) MS^3 spectrum of the major product from (a). (c) MS^2 spectrum of singly charged dimagnesium complex of disulfide linked AARAAACAA dimer showing a major product from elimination of H_2S_2 and a minor product from H_2S elimination (d) MS^3 spectrum of the major product from (c). Arrows indicate the ion peaks being isolated and collisionally activated.

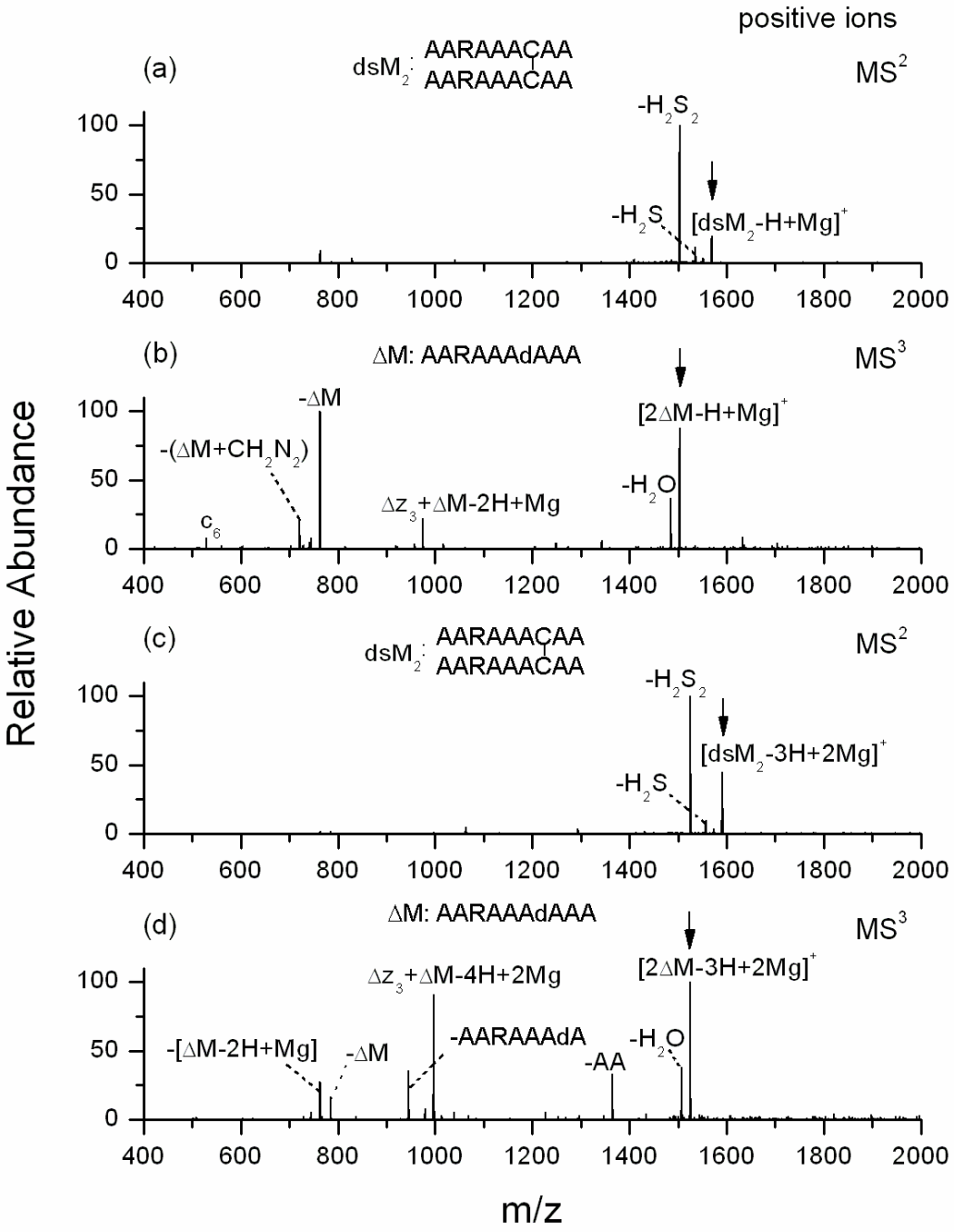
positive ions
(a)
dsM2: AARAAACAA
AARAAACAA
MS2
-H2S2
-H2S
[dsM2-H+Mg]+
(b)
ΔM: AARAAAdAAA
MS3
-ΔM
[2ΔM-H+Mg]+
-(ΔM+CH2N2)
-H2O
ΔZ3+ΔM-2H+Mg
c6
(c)
dsM2: AARAAACAA
AARAAACAA
MS2
-H2S2
[dsM2-3H+2Mg]+
-H2S
(d)
ΔM: AARAAAdAAA
MS3
ΔZ3+ΔM-4H+2Mg
[2ΔM-3H+2Mg]+
-[ΔM-2H+Mg]
-ΔM
-AARAAAdA
-H2O
-AA
Relative Abundance
m/z

Figure 6. (a) MS^2 spectrum of singly charged monocalcium complex of disulfide linked AARAAACAA dimer showing a major product from elimination of H_2S_2 and three minor products from H_2S elimination and disulfide bond cleavages. (b) MS^3 spectrum of the major product from (a). (c) MS^2 spectrum of singly charged dicalcium complex of disulfide linked AARAAACAA dimer showing an exclusive product from elimination of H_2S_2. (d) MS^3 spectrum of the product from (c). Arrows indicate the ion peaks being isolated and collisionally activated.

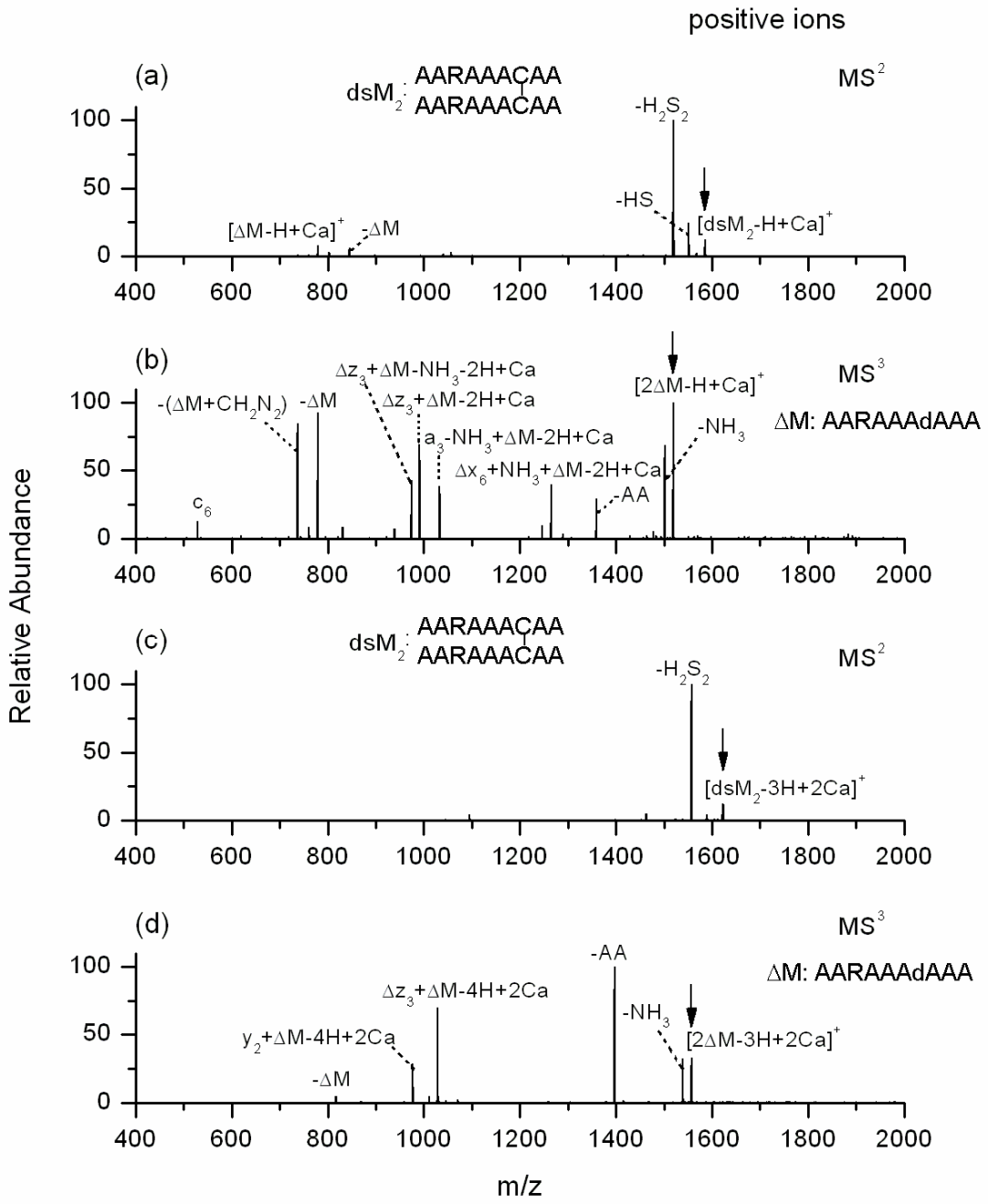
positive ions
(a)
dsM2: AARAAACAA
AARAAACAA
MS2
-H2S2
-HS
[dsM2-H+Ca]+
[ΔM-H+Ca]+
-ΔM
(b)
MS3
ΔM: AARAAAdAAA
Δz3+ΔM-NH3-2H+Ca
[2ΔM-H+Ca]+
-(ΔM+CH2N2)
-ΔM
Δz3+ΔM-2H+Ca
-NH3
a3-NH3+ΔM-2H+Ca
Δx6+NH3+ΔM-2H+Ca
-AA
c6
(c)
dsM2: AARAAACAA
AARAAACAA
MS2
-H2S2
[dsM2-3H+2Ca]+
(d)
MS3
ΔM: AARAAAdAAA
-AA
Δz3+ΔM-4H+2Ca
-NH3
y2+ΔM-4H+2Ca
[2ΔM-3H+2Ca]+
-ΔM
Relative Abundance
m/z

monomeric peptide with Cys converted to a disulfide, respectively. In addition, the product from the elimination of H_2S is also observed. As seen in Figure 4d, the process involving elimination of H_2S_2 yields the dominant product observed in the CID spectrum of the trisodiated peptide. The MS^3 spectrum of the product from the elimination of H_2S_2 exhibits selective backbone cleavage of the monomeric product peptide (Figure 4e). Other than the monomeric dissociation of the neutral monosodiated AARAAAdAAA, the product at m/z 1019.4 comprises a z-type fragment (z_3) formed by cleavage at the dehydroalanine (dA) residue. In addition, a minor product resulting from the elimination of C-terminus dialanine (AA) is observed at m/z 1387.5. Observed CID pathways of trisodiated MP2 cation are summarized in Scheme 2.

Similar to the low energy CID of the multiply sodiated peptide, highly selective eliminations are observed from the singly charged magnesium and calcium bound peptides via low energy CID (Figures 5 and 6). The products resulting from the elimination of H_2S_2 are observed as the exclusive products from MS^2 spectra (Figures 5a, c and 6a, c) of both singly charged mono- and di-metal bound peptide ions. The MS^3 of the product ions also yield z_3 fragments as the dominant product (Figures 5b, d and 6b, d).

2.4.4. Metal Complexes of LVP and OT. The CID products of protonated, sodiated, and magnesium and calcium bound LVP and OT are listed in Table 1. Highly specific elimination of H_2S_2 is observed from the low energy CID of both singly charged LVP and OT ionized by attachment of divalent magnesium or calcium cations. Figure 7 compares the CID pathways of the singly charged LVP complexes of magnesium cation (Figure 7a-c) and calcium cation (Figure 7d-f). Mass spectra of singly charged cationic magnesium bound LVP and calcium bound LVP are shown in Figures 7a and 7d, respectively.

Table 1. The CID products of protonated, sodiated, magnesium and calcium bound LVP and OT

Parent ion	Major CID process/products	Minor CID process/products
$[dsLVP+H]^+$	$-NH_3$, b_6, b_6-NH_3	$-H_2S$, b_8, b_8-NH_3
$[dsLVP+Na]^+$	$-NH_3$, b_6, b_6-NH_3	$-H_2S_2$, b_8
$[dsLVP-H+Mg]^+$	$-H_2S_2$	$-NH_3$, z_5+S, b_5, a_4-CH_3S, a_4-CH_3S-NH_3
$[\Delta_2LVP-H+Mg]^+$	Δz_5, Δb_5	Δz_5-NH_3, Δc_5, Δc_4
$[dsLVP-H+Ca]^+$	$-H_2S_2$	$-NH_3$, z_5+S, Δz_5
$[\Delta_2LVP-H+Ca]^+$	Δz_5, $\Delta_2 c_8$, Δb_5	
$[dsOT+H]^+$	$-NH_3$, b_6	$-H_2S$, b_8
$[dsOT+Na]^+$	$-NH_3$, b_6	$-H_2S_2$, -CO, a_6
$[dsOT-H+Mg]^+$	$-H_2S_2$	$-NH_3$, z_5-S, z_5+S, b_6, a_6, a_4-CH_3S,
$[\Delta_2OT-H+Mg]^+$	$-NH_3$, Δz_5, Δb_6, Δb_5,	Δc_5, Δc_4
$[dsOT-H+Ca]^+$	$-H_2S_2$	z_5+S, Δz_5
$[\Delta_2OT-H+Ca]^+$	-Pro, $-NH_3$, Δz_5, Δb_5	Δc_5, Δc_4

Figure 7. (a) ESI-MS spectrum of LVP with magnesium dichloride in positive mode. (b) CID spectrum of singly charged magnesium bound LVP ion. (c) MS^3 of product from elimination of H_2S_2 from (b). (d) ESI-MS spectrum of LVP with calcium dichloride in positive mode. (e) CID spectrum of singly charged calcium bound LVP ion. (f) MS^3 of product from elimination of H_2S_2 from (e). Arrows indicate the ion peaks being isolated and collisionally activated.

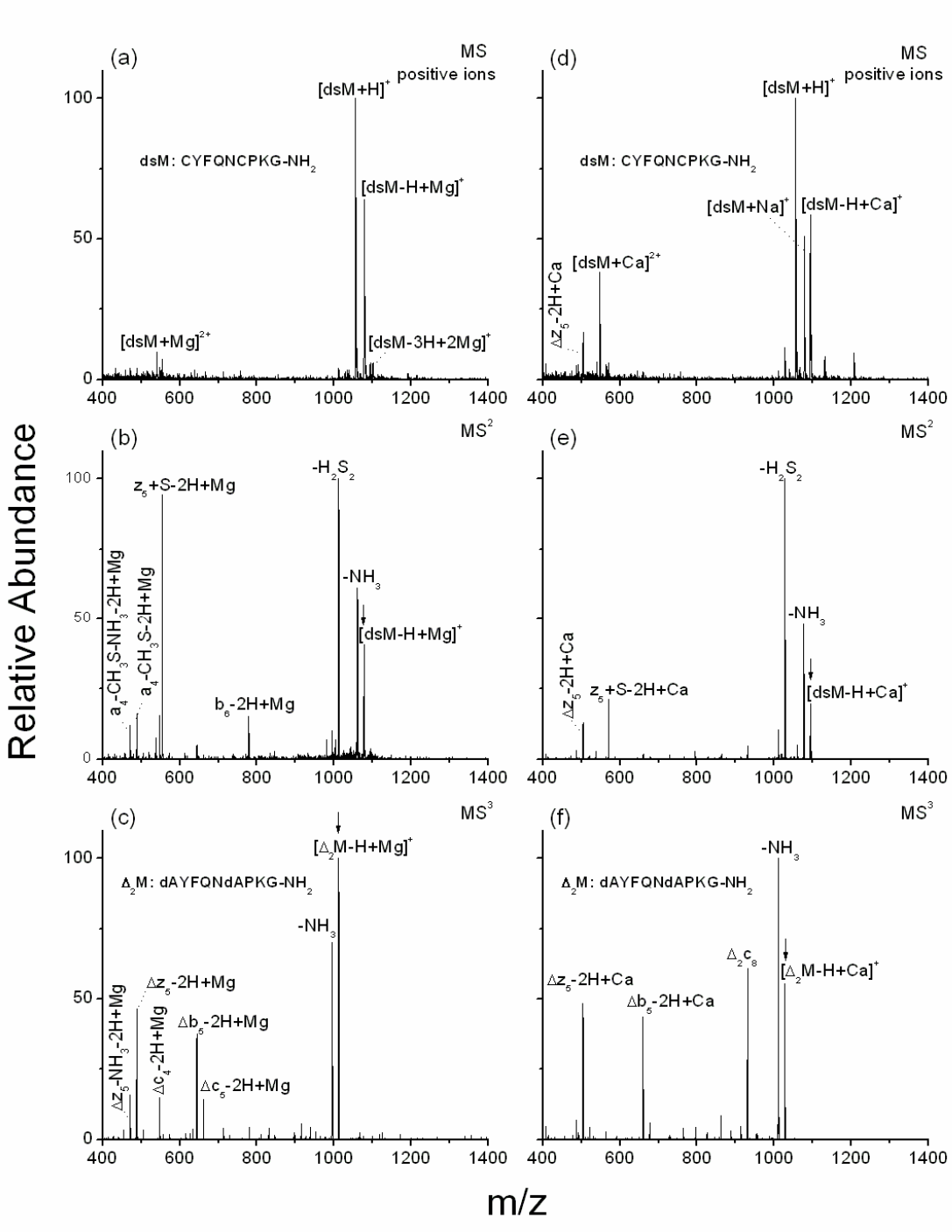
(a)
MS
positive ions
[dsM+H]+
dsM: CYFQNCPKG-NH2
[dsM-H+Mg]+
[dsM+Mg]2+
[dsM-3H+2Mg]+
(d)
MS
positive ions
[dsM+H]+
dsM: CYFQNCPKG-NH2
[dsM+Na]+
[dsM-H+Ca]+
[dsM+Ca]2+
ΔZ5-2H+Ca
(b)
MS2
z5+S-2H+Mg
-H2S2
-NH3
[dsM-H+Mg]+
a4-CH3S-NH3-2H+Mg
a4-CH3S-2H+Mg
b6-2H+Mg
(e)
MS2
-H2S2
-NH3
[dsM-H+Ca]+
ΔZ5-2H+Ca
z5+S-2H+Ca
(c)
MS3
[Δ2M-H+Mg]+
Δ2M: dAYFQNdAPKG-NH2
-NH3
ΔZ5-2H+Mg
ΔZ5-NH3-2H+Mg
Δc4-2H+Mg
Δb5-2H+Mg
Δc5-2H+Mg
(f)
MS3
-NH3
Δ2M: dAYFQNdAPKG-NH2
Δ2c8
[Δ2M-H+Ca]+
ΔZ5-2H+Ca
Δb5-2H+Ca
Relative Abundance
m/z

CID of these ions yields products resulting from the elimination of H_2S_2 with high specificity (Figures 7b and 7e). In addition, z_5 fragment products with Cys converted to a disulfide are observed in both mass spectra. MS^3 spectra of both magnesium and calcium bound product peptides from the elimination of H_2S_2 show the common major fragments of Δz_5 and Δb_5 (Figures 7c and 7f). The peptides OT and LVP are similar, differing only in two residues. Not surprisingly, the MS^n spectra of the singly charged divalent metal (Mg^{2+} and Ca^{2+}) complexes of OT and LVP exhibit nearly identical dissociation pathways.

CID spectra of the protonated and sodiated LVP and OT peptides were also examined. Both exhibit major products resulting from the elimination of NH_3 and formation of b_6 fragments. An abundant product from the elimination of H_2S_2 is observed in CID spectra of singly sodiated LVP and OT. Minor products comprising the b_6-NH_3 fragment and a_6 fragment are observed in the CID spectra of the protonated and sodiated LVP.

2.4.5. Sodiated Peptides from Pepsin Digest of Insulin. The ESI mass spectrum shows 8 major ion peaks from the pepsin digest of insulin (Figure 8). The masses and segments of observed peptic digest peptides of insulin ions are listed in Table 2 along with observed selective elimination of H_2S_2 from singly sodiated species. The observed segments are in excellent agreement with earlier published analyses of the peptic digest of insulin.[43,44] CID of singly charged protonated and sodiated peptides was performed. Figure 9 shows MS^2 spectra of the disulfide linked peptide pair at m/z 1537.6, NYCN/LVCGERGFF, found in the mass spectrum of peptic digests of insulin. CID of the singly charged protonated ion (Figure 9a) mainly results in dehydration (-18 mass units). In contrast, CID of the singly sodiated dipeptide NYCN/LVCGERGFF at m/z 1559.5 yields a major product resulting from H_2S_2 elimination (Figure 9b).

Figure 8. ESI-MS of pepsin digest of insulin in positive mode. Structure of insulin is shown with amino acid numbering of the two chains.

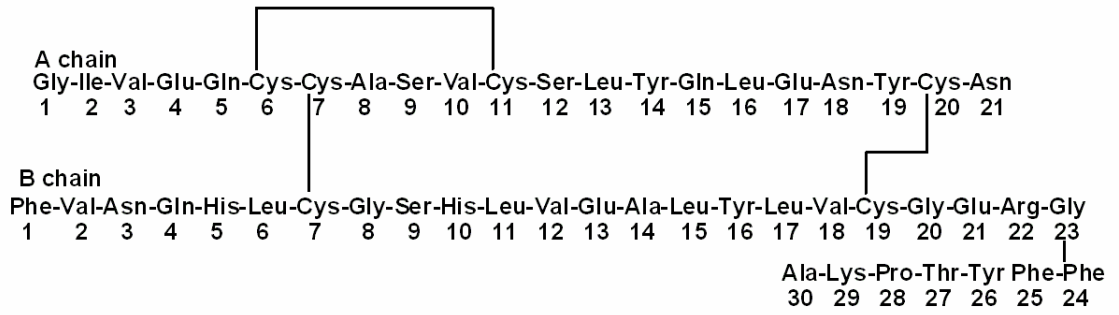
A chain
Gly-Ile-Val-Glu-Gln-Cys-Cys-Ala-Ser-Val-Cys-Ser-Leu-Tyr-Gln-Leu-Glu-Asn-Tyr-Cys-Asn
1 2 3 4 5 6 7 8 9 10 11 12 13 14 15 16 17 18 19 20 21
B chain
Phe-Val-Asn-Gln-His-Leu-Cys-Gly-Ser-His-Leu-Val-Glu-Ala-Leu-Tyr-Leu-Val-Cys-Gly-Glu-Arg-Gly
1 2 3 4 5 6 7 8 9 10 11 12 13 14 15 16 17 18 19 20 21 22 23
Ala-Lys-Pro-Thr-Tyr Phe-Phe
30 29 28 27 26 25 24

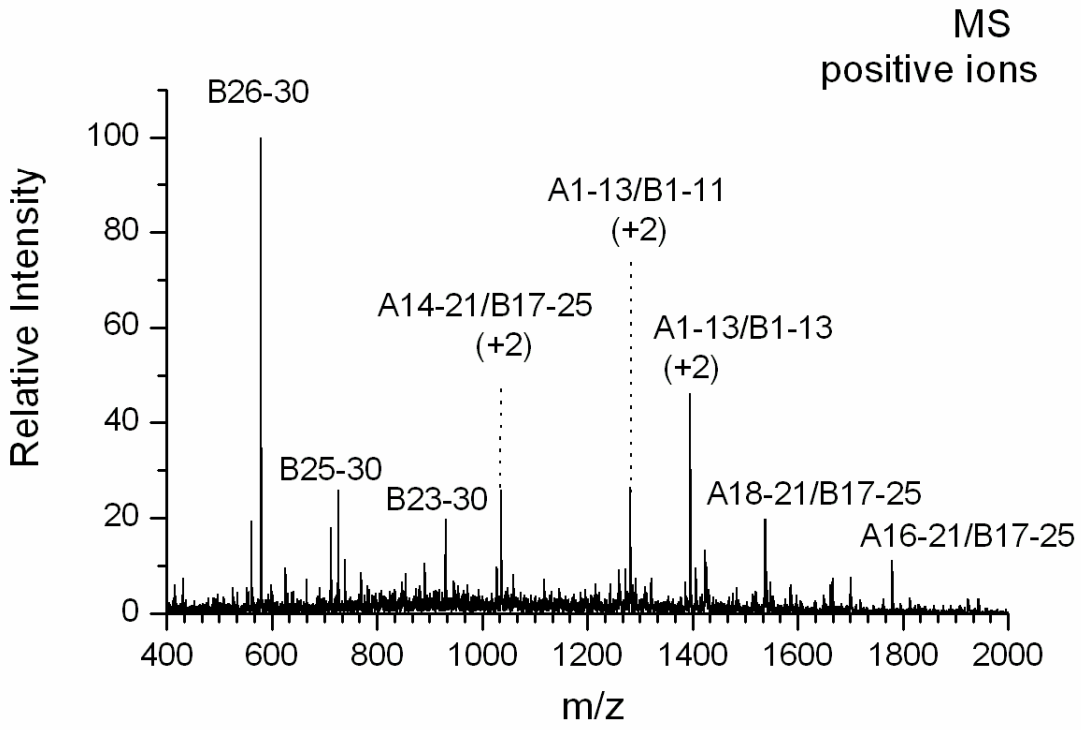
MS
positive ions
B26-30
A1-13/B1-11
(+2)
A14-21/B17-25
(+2)
A1-13/B1-13
(+2)
B25-30
B23-30
A18-21/B17-25
A16-21/B17-25
Relative Intensity
100
80
60
40
20
0
400
600
800
1000
1200
1400
1600
1800
2000
m/z

Table 2. Major peptide ions in the mass spectrum of the 6 hours pepsin digest of insulin

Segment[a,b]	Sequence[b]	Charge state	m/z (Protonated)	m/z (Sodiated)[c]	Number of H_2S_2 eliminated[d]
B26-30	YTPKA	+1	579.3	601.4	0
B25-30	FYTPKA	+1	726.4	748.5	0
B23-30	GFFYTPKA	+1	931.2	953.3	0
A14-21/B17-25	YQLENYCN/ LVCGERGFF	+2	1036.4	1048.4	0[e]
A1-13/B1-11	GIVEQCCASVCSL/ FVNQHLCGSHL	+2	1281.6	1292.5	2
A1-13/B1-13	GIVEQCCASVCSL/ FVNQHLCGSHLVE	+2	1395.5	1406.5	2
A18-21/B17-25	NYCN/ LVCGERGFF	+1	1537.6	1559.5	1
A16-21/B17-25	LENYCN/ LVCGERGFF	+1	1779.5	1801.5[f]	-[f]

[a]Amino acid numbering for the two chains is shown in Figure 8. [b]Peptide pair with disulfide linkage is indicated with "/." [c]Singly sodiated ion. [d]CID of singly sodiated ion. [e]Major product observed is dehydration of singly sodiated peptide. [f]Due to low intensity of this fragment the singly sodiated species was not observed in sufficient abundance for MS^2 analysis.

Figure 9. (a) MS^2 spectrum of singly charged protonated peptic digest fragment from insulin, NYCN/LVCGERGFF, at m/z 1537.5. (b) MS^2 spectrum of singly charged monosodiated peptic digest fragment from insulin, NYCN/LVCGERGFF, at m/z 1559.5, showing a major product involving elimination of H_2S_2 and four minor products from disulfide bond cleavages. Arrows indicate the ion peaks being isolated and collisionally activated.

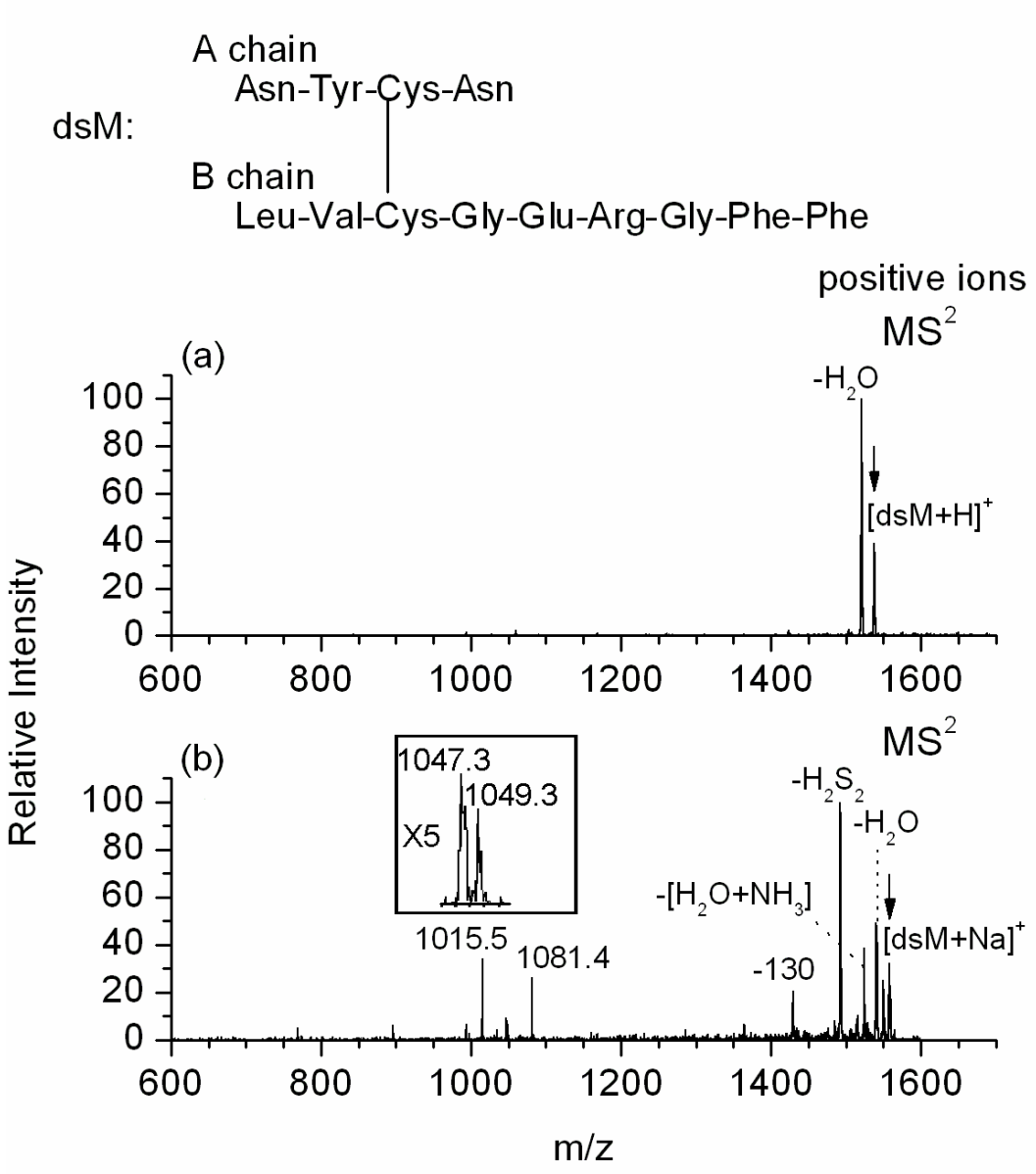
A chain
Asn-Tyr-Cys-Asn
dsM:
B chain
Leu-Val-Cys-Gly-Glu-Arg-Gly-Phe-Phe
positive ions
MS2
(a)
-H2O
[dsM+H]+
(b)
1047.3
1049.3
X5
1015.5
1081.4
-H2S2
-H2O
-[H2O+NH3]
-130
[dsM+Na]+
Relative Intensity
m/z

The observed elimination of H_2S_2 indicates the presence of a disulfide linkage in the peptide. In addition, products separated by 66 mass units at m/z 1015.5 and 1081.4 result from the two possible S-C bond cleavage processes and minor products at m/z 1047.3 and m/z 1049.3 are the result of the S-S bond cleavage to yield a thial and thiol, respectively. These combined results demonstrate the presence of a disulfide linkage between two peptic digest fragments.

2.5. Discussion

Remarkably, all singly charged sodiated and alkaline earth metal (Mg^{2+} and Ca^{2+}) bound peptide cations investigated in the present study exhibit S-C bond cleavage as a prominent low energy CID pathway. This results in the selective elimination of H_2S_2 and H_2S from the peptides containing disulfide linkage and MP1 with Cys, respectively. To understand the mechanisms of the observed selective S-C bond eliminations, we first consider the driving force for the selective S-C bond cleavage over S-S bond cleavage.

2.5.1. Selective S-C bond Cleavage Processes Involving Sodiated Cystine. The CID spectra of the series of sodiated cystine cations exhibit three products of particular interest, two involving S-S bond cleavage and one resulting from S-C bond cleavage (Figure 2b-d). It is notable that there are two competitive products involving S-S bond cleavage. Lioe and O'Hair demonstrated symmetric S-S bond cleavage from the CID of protonated cystine and its derivatives.[12] They proposed a charge directed neighboring group mechanism for the observed symmetric S-S bond cleavage process (Scheme 3). In contrast, the present study demonstrates that CID of the sodiated cystine cations results in the asymmetric S-S bond cleavage. The relative abundance of the product from the loss of 119 mass units ($C_3H_5NO_2S$) increases along with the number of sodium cations

Scheme 3. A charge directed neighboring group mechanism of protonated cystine for the cleavage of S-S bond proposed by Lioe and O'Hair.[12]

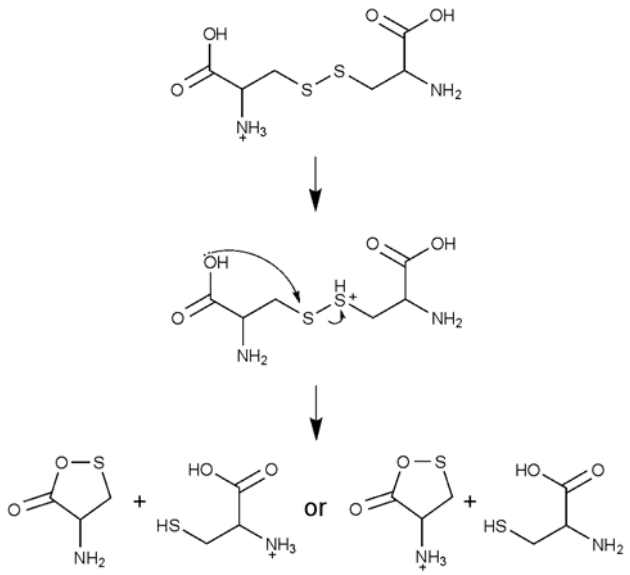

(Figure 2b-d). We propose that the product from the loss of 119 mass units ($C_3H_5NO_2S$) is formed via a neighboring group process[12] while the product from the loss of 121 mass units (cysteine) is expected to form via a salt bridge mechanism[28,45] (Scheme 1). Lee et al. previously demonstrated selective cleavage at aspartic acid residues in sodiated peptides and suggested that the sodium cation stabilized a salt bridge intermediate.[28] We propose that the dominant product of the singly sodiated cystine cation, resulting from the loss of 121 mass units (Figure 2b), is from a salt bridge intermediate, which is stabilized by sodium cation. As all the acidic protons are replaced by sodium cations in the triply sodiated cystine cation, the formation of a salt bridge intermediate is no longer an option. Under these conditions we propose that S-S bond cleavage is dominated by a charge directed neighboring group process. Consequently, the products involving loss of 119 mass units is the solo process resulting from S-S bond cleavage when triply sodiated cystine is subjected to low energy CID (Figure 2d). Collisional activation of sodiated

Figure 10. Reaction coordinate diagrams showing relative energies in kcal/mol for S-S bond cleavage (left side) and S-C bond cleavage (right side) of disodiated cystine cation at the B3LYP/6-311G** level, including zero-point correction obtained at the same scaled level. Barrier heights are not known. Optimized geometries for corresponding states are obtained at the same scaled level. The reaction mechanism of each numbered step is shown in Scheme 1.

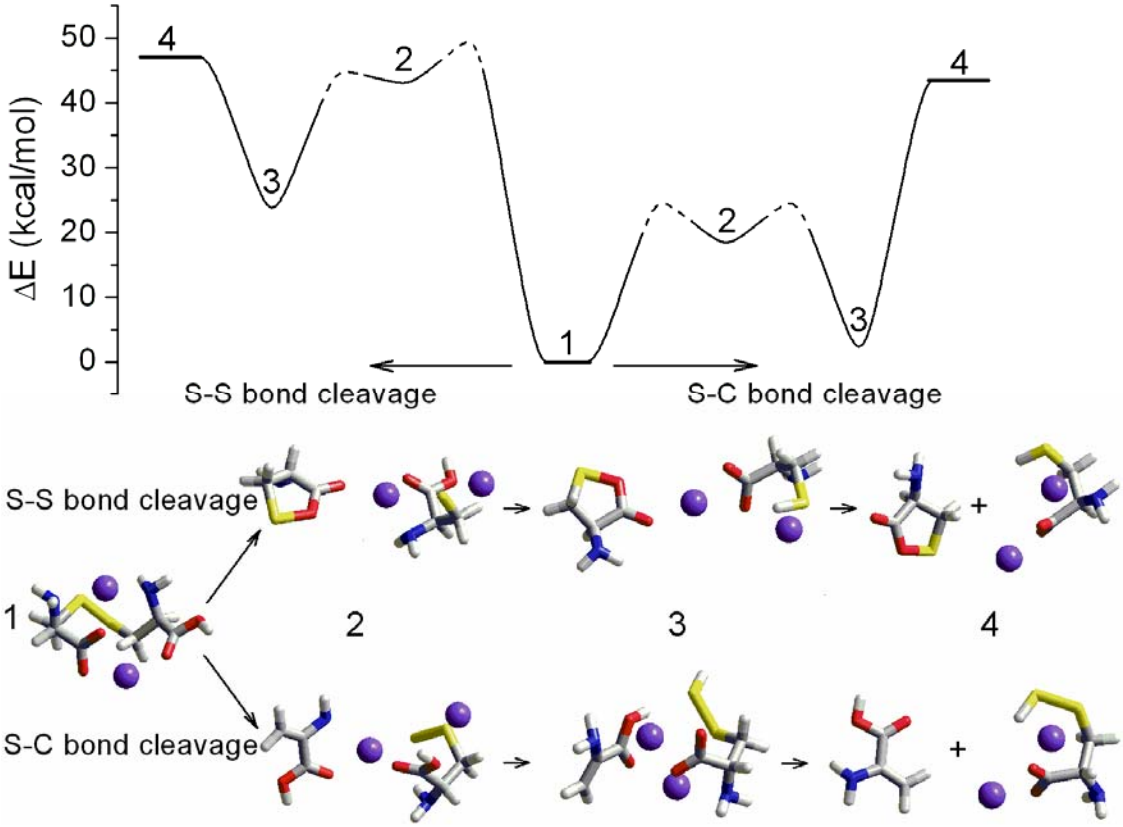
ΔE (kcal/mol)
50
40
30
20
10
0
4
2
3
1
2
3
4
S-S bond cleavage
S-C bond cleavage
S-S bond cleavage
S-C bond cleavage
1
2
3
4
+
+

cystine cations results in an increased preference for S-C bond cleavage over S-S bond cleavage as the number of sodium ions in the complex increases (Figure 2c-d). The DFT calculated changes of electronic energy (ΔE) associated with cleavages involving S-S and S-C bonds in the singly charged disodiated cystine cation are shown in Figure 10, along with the optimized geometries of the corresponding intermediates. As seen in Figure 10, the overall reaction process involving S-C bond cleavage is energetically favored by ~3 kcal/mol. It is notable that intermediate species associated with S-C bond cleavage are energetically more favored by ~23 kcal/mol when compared to intermediates involved in cleavage of the S-S bond. The formation of cysteine disulfide from S-C bond cleavage is initiated by enolization of cystine. The cysteine product from S-S bond cleavage results from an initial nucleophilic attack of the carboxylate group adjacent to the disulfide linkage. Interaction of a sodium cation with the disulfide group renders S-C bond cleavage more energetically favorable. This is consistent with the observation that S-C bond cleavage increases relating to S-S bond cleavage as the number of sodium ions in the complex increases (Figures 2c and 2d).

2.5.2. Selective S-C bond Cleavage Processes Involving Metal Complexes of Model Peptides. The present study demonstrates that singly charged sodiated and alkaline earth metal bound disulfide linked peptide cations readily undergo selective elimination of H_2S_2 via CID. It is notable that the total charge of the metal peptide complexes investigated in the present study is +1. With two or more sodium ions or a divalent alkaline earth metal a +1 charge of the complex suggests that the peptide is negatively charged. This is likely responsible for some of the similarities between our work and the earlier study of anionic peptides reported by Bowie and co-workers.[15,18,46] They observed selective losses of H_2S and H_2S_2 from CID of peptides with Cys and peptides with

Scheme 4. The dissociation mechanisms of anionic peptide CGGCG with intramolecular disulfide bond via enolization at Cys backbone proposed by Bilusich et al..[15] Optimized geometries and energy changes for corresponding labeled states of CGGCG are shown in Figure 11.

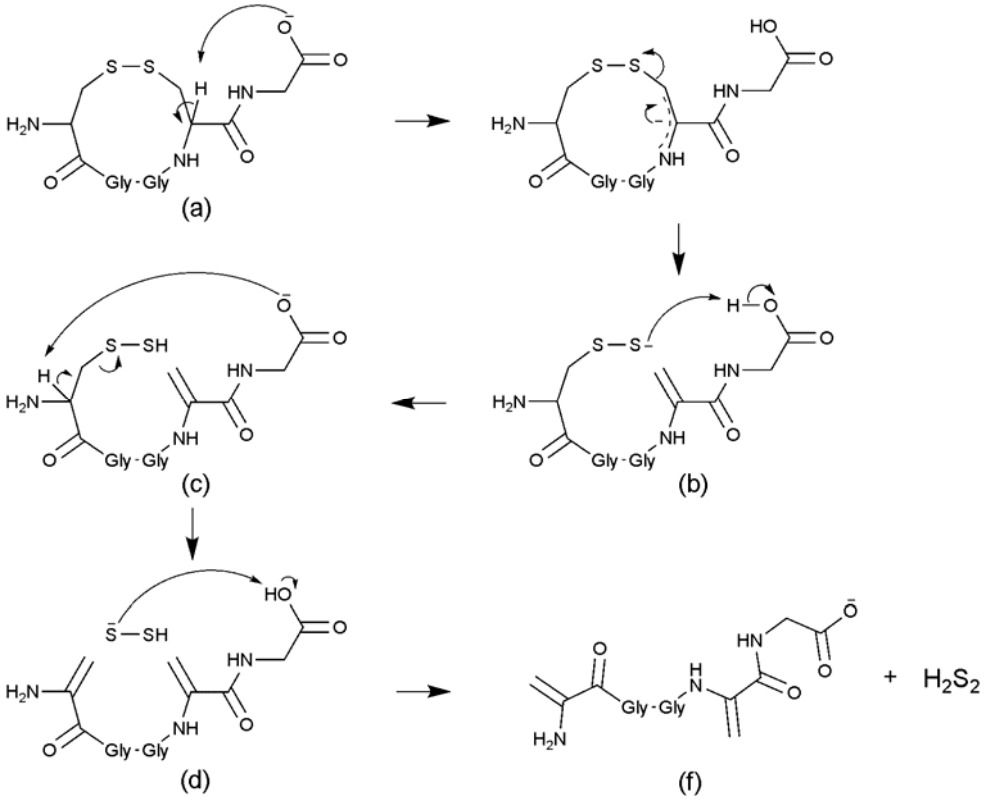

intramolecular disulfide bond, respectively.[15,46] They have proposed dissociation mechanisms that are initiated by enolate anion formation at Cys (Scheme 4).[15]

We propose that selective eliminations of H_2S and H_2S_2 from singly charged collisionally activated metal complex peptides is initiated by formation of an enolate anion at the Cys residue (Scheme 5). The z_3 fragment, which contains dehydroalanine, from MS^3 of the disulfide linked MP2 suggests that the hydrogens attached to the sulfur atoms originated from the α-carbon of Cys as a result of the enolation process (Figures 5b, d and 6b, d; Scheme 5). These selective dissociations are most prominent with multiply

Scheme 5. Proposed H_2S_2 elimination mechanisms of singly charged cationic divalent metal (M^{2+}) bound peptide CGGCG with intramolecular disulfide bond. Optimized geometries and energy changes for corresponding numbered states of magnesium bound CGGCG are shown in Figure 11.

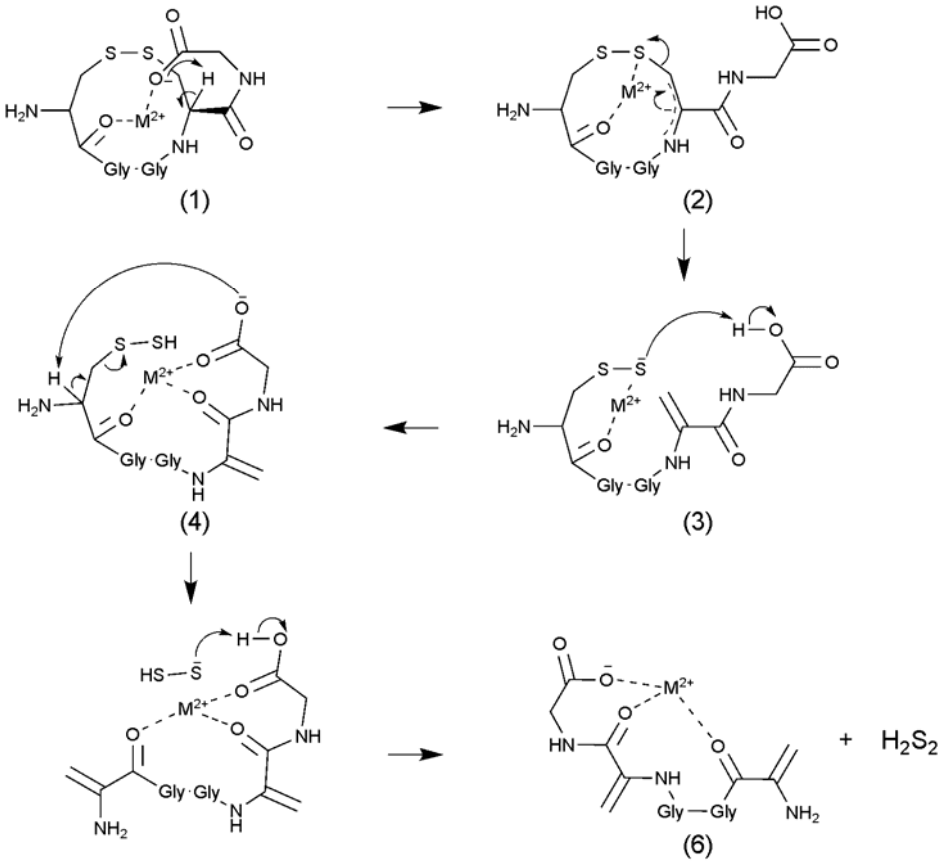

sodiated peptides, where the peptides possess one or more negative charges (Figures 3 and 4).

In addition to the negative charge of a peptide, metal cations play a key role in the selective elimination of H_2S and H_2S_2. As observed from the studies of MP1 and MP2, CID of the peptides with multiple metal cations (Figures 3-6) shows more prominent loss of H_2S and H_2S_2 than is observed with the single metal bound peptide. DFT calculations have been performed to address the energetic comparison for the elimination of H_2S_2 between the singly charged CGGCG anion with an intramolecular disulfide bond and the

singly charged magnesium complex cation of the corresponding peptide. Calculated energetics for the elimination are shown in Figure 11 with DFT optimized geometries. As seen in Figure 11, the H_2S_2 elimination process of anionic CGGCG is endothermic by ~6 kcal/mol. However, the process is overall exothermic when Mg^{2+} is present in the complex. Both magnesium bound CGGCG cation and anionic CGGCG initiate S-C bond cleavage via backbone enolization at the C-terminal Cys. This process is energetically favored by ~3 kcal/mol for the magnesium bound CGGCG. However, the Cys backbone enolization of deprotonated CGGCG is energetically unfavorable and concomitant S-C bond cleavage is observed with enolization of the peptide anion without a metal cation.

The formation of intermediate products from the magnesium bound CGGCG cation is energetically favored by ~25 - 30 kcal/mol through the elimination process while the formation of intermediates from the anionic CGGCG is favored by ~5 - 15 kcal/mol. As seen from the optimized structures in Figure 11, the intermediates from anionic CGGCG are generally stabilized via intramoleculaFr hydrogen bonds. In addition to hydrogen bond interactions, ionic interactions between magnesium cation and polar functional groups including the negatively charged carboxylate group enhance the stability of the intermediates from the magnesium bound CGGCG cation.

2.5.3. Selective Elimination of H_2S_2 from Metal Complexes of Peptides Containing an Intramolecular Disulfide Linkage. The C-termini of both LVP and OT are amides rather than more usual carboxylic acid. It is notable that the singly charged alkaline earth metal (Mg^{2+} and Ca^{2+}) complexes of LVP and OT are readily observed in the mass spectra even though there is no acidic functional group in the peptide. CID of singly protonated and sodiated LVP and OT yields a common b_6 fragment. The cyclic structure

Figure 11. Reaction coordinate diagrams showing relative energies in kcal/mol for the elimination of H_2S_2 from deprotonated anionic CGGCG (left side) and magnesium bound cationic CGGCG (right side) at the B3LYP/LACVP level, including zero-point correction obtained at the same scaled level. Barrier heights are not known. Optimized geometries are obtained at the same scaled level. The geometries for reactants, products, and intermediates are shown below the diagram. The reaction mechanism of each labeled and numbered step is shown in Schemes 4 and 5, respectively.

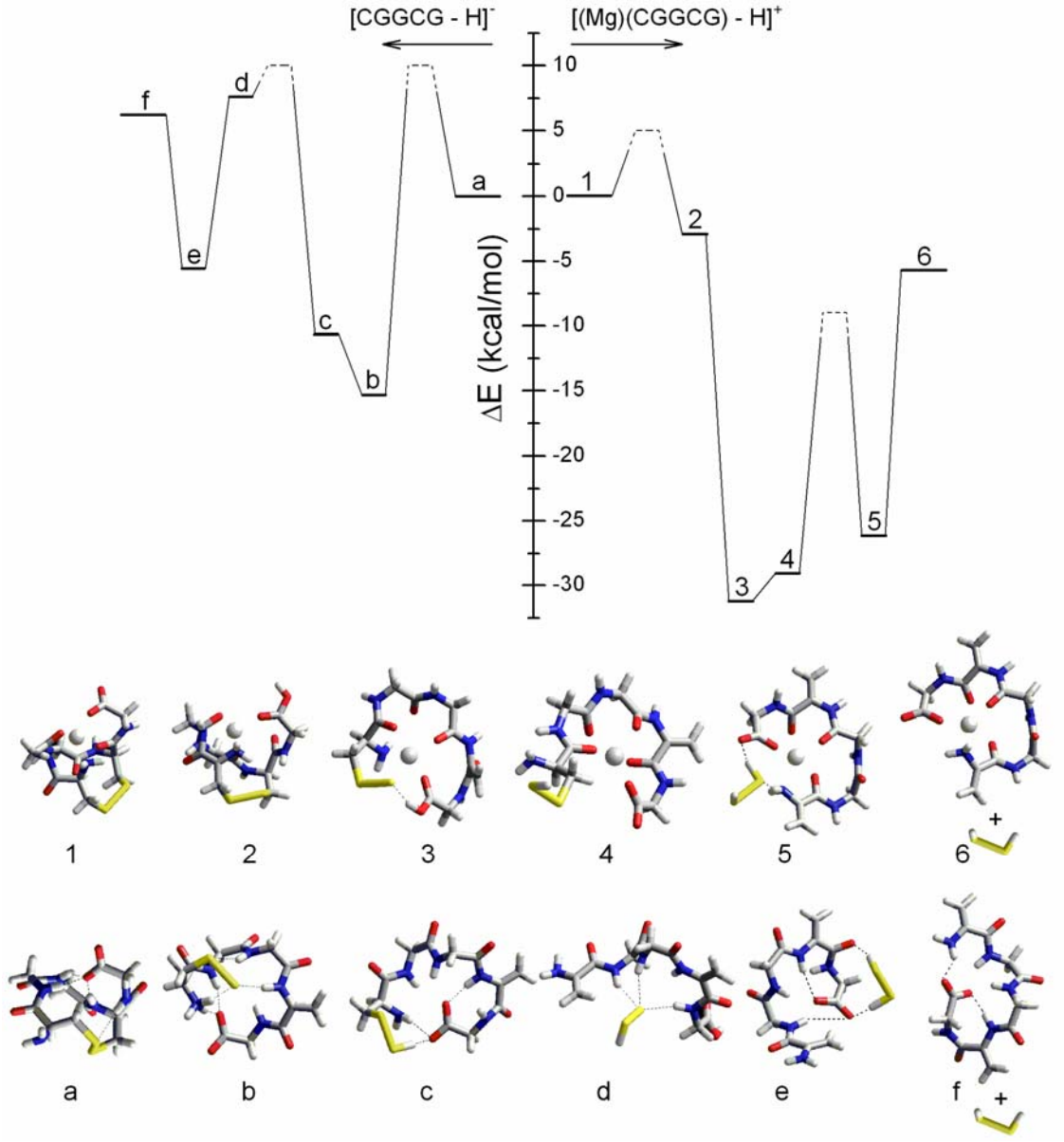
[CGGCG - H]⁻
[(Mg)(CGGCG) - H]⁺
ΔE (kcal/mol)
10
5
0
-5
-10
-15
-20
-25
-30
a
b
c
d
e
f
1
2
3
4
5
6
+
+

Scheme 6. The γ backbone cleavage of anionic peptides at an asparagine residue.[47]

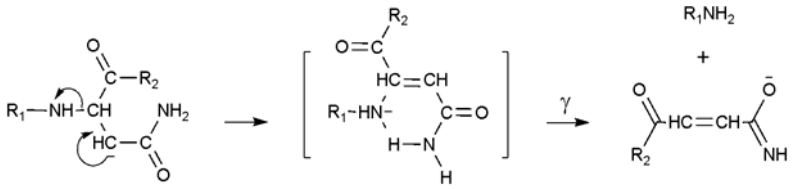

of the b_6 fragment with an intramolecular disulfide linkage renders difficult the determination of additional sequence and structural (i.e., location of disulfide linkage) information of a peptide (Table 1).

CID of the singly charged alkaline earth metal (Mg^{2+} and Ca^{2+}) bound LVP (Figures 7b and 7e; Table 1) and OT yields major products resulting from the selective elimination of H_2S_2. The MS^3 spectra of these products show two major fragments, Δz_5 and Δb_5. The observed Δz_5 fragments result from γ backbone cleavage of anionic peptides (Scheme 6), which is a characteristic dissociation pathways at an asparagine residue.[47] This observation provides sequence information in the region of the peptide originally bridged by the disulfide bond in LVP, in contrast to the results obtained with the protonated peptide. In addition, Δb_5 fragments reveal the location of the Cys residue which forms the disulfide bond in the peptide.

2.5.4. Identifying a Disulfide Linkage using Selective Elimination of H_2S_2 from Sodium Complexes of Peptides Generated from a Pepsin Digest of Insulin. In order to provide an example of the utility of the selective elimination of H_2S_2 for identifying peptides with a disulfide linkage in complex mixtures, we examined the peptic digest of insulin. Insulin is a small model protein comprising two peptide chains with three closely located disulfide linkages (Figure 1). As seen in Figure 9a, CID of the protonated peptide at m/z 1537.6 mainly results in the facile elimination of water and provides no useful data

relating to the presence of a disulfide linkage. However, CID of the singly charged sodiated species at m/z 1559.5 clearly exhibits the presence of disulfide linkage in the peptide via the selective elimination of H_2S_2 (Figure 9b). The cation at m/z 1559.5 is the singly sodiated dipeptide, NYCN/LVCGERGFF, linked via an intermolecular disulfide bond. As discussed above, CID of the sodiated cation also yields products resulting from cleavages of S-S and S-C bonds at the intermolecular disulfide linkage in analogy with the results for the model peptide in Figure 4. In all cases the sodium ion is retained with larger of the two peptide fragments, LVCGERGFF.

By scanning MS^2 of singly sodiated peptic digest components for loss of 66 mass units (H_2S_2) it is possible to identify peptide fragments with disulfide linkages. Once the existence of the disulfide linkage in the peptide is determined via selective elimination of H_2S_2, further activation and dissociation of the product ion(s) may provide additional sequence information revealing the position of the disulfide linkage in the peptide, such as observed in the case of LVP and OT in the present study. The elimination of H_2S_2 replaces the original cysteine residue involved in the linkage with a dehydroalanine, thus distinguishing it from other cysteine not involved in disulfide linkages.

2.6. Conclusion

Collisional activation of singly charged sodium and alkaline earth metal complexes of peptide cations containing disulfide bonds results in highly selective elimination of H_2S_2 in the gas phase. Further activation of the product yields sequence information in the region previously short circuited by the disulfide bond. The selective elimination is initiated from a metal stabilized enolate anion at Cys, with the intermediate products

being further stabilized by the cation. This observation provides the possibility of simply and rapidly identifying an intra or an intermolecular disulfide linkage in peptides.

2.7. Acknowledgment

The research described in this paper was carried out at the Beckman Institute and the Noyes Laboratory of Chemical Physics at the California Institute of Technology. We appreciate the support provided by the Beckman Institute Mass Spectrometry Resource Center, and the Planetary Science and Life Detection section, Jet Propulsion Laboratory, California Institute of Technology. Partial support was also provided by the National Science Foundation (NSF) under grant No. CHE-0416381. The authors greatly appreciate critical discussions with Hyungjun Kim in the Beckman Institute Materials and Process Simulation Center relating to the computational modeling.

2.8. References

(1) Thornton, J. M. *J. Mol. Biol.* **1981**, *151*, 261-287.

(2) Gorman, J. J.; Wallis, T. P.; Pitt, J. J. *Mass Spectrom. Rev.* **2002**, *21*, 183-216.

(3) Chelius, D.; Wimer, M. E. H. *J. Am. Soc. Mass. Spectrom* **2006**, *17*, 1590-1598.

(4) Biemann, K.; Scoble, H. A. *Science* **1987**, *237*, 992-998.

(5) Mann, M.; Jensen, O. N. *Nat. Biotechnol.* **2003**, *21*, 255-261.

(6) Resing, K. A.; Johnson, R. S.; Walsh, K. A. *Biochemistry* **1995**, *34*, 9477-9487.

(7) Gibson, B. W.; Cohen, P. *Method Enzymol.* **1990**, *193*, 480-501.

(8) Huddleston, M. J.; Annan, R. S.; Bean, M. F.; Carr, S. A. *J. Am. Soc. Mass Spectrom.* **1993**, *4*, 710-717.

(9) Clauser, K. R.; Hall, S. C.; Smith, D. M.; Webb, J. W.; Andrews, L. E.; Tran, H. M.; Epstein, L. B.; Burlingame, A. L. *Proc. Natl. Acad. Sci. U. S. A.* **1995**, *92*, 5072-5076.

(10) Qin, J.; Chait, B. T. *Anal. Chem.* **1997**, *69*, 4002-4009.

(11) Reid, G. E.; Roberts, K. D.; Kapp, E. A.; Simpson, R. J. *J. Proteome Res.* **2004**, *3*, 751-759.

(12) Lioe, H.; O'Hair, R. A. J. *J. Am. Soc. Mass. Spectrom* **2007**, *18*, 1109-1123.

(13) Stephenson, J. L.; Cargile, B. J.; McLuckey, S. A. *Rapid Commun. Mass Spectrom.* **1999**, *13*, 2040-2048.

(14) Wells, J. M.; Stephenson, J. L.; McLuckey, S. A. *Int. J. Mass Spectrom.* **2000**, *203*, A1-A9.

(15) Bilusich, D.; Maselli, V. M.; Brinkworth, C. S.; Samguina, T.; Lebedev, A. T.; Bowie, J. H. *Rapid Commun. Mass Spectrom.* **2005**, *19*, 3063-3074.

(16) Chrisman, P. A.; McLuckey, S. A. *J. Proteome Res.* **2002**, *1*, 549-557.

(17) Zhou, J.; Ens, W.; Poppeschriemer, N.; Standing, K. G.; Westmore, J. B. *Int. J. Mass Spectrom. Ion Process.* **1993**, *126*, 115-122.

(18) Bilusich, D.; Bowie, J. H. *Curr. Anal. Chem.* **2006**, *2*, 341-352.

(19) Zubarev, R. A.; Kruger, N. A.; Fridriksson, E. K.; Lewis, M. A.; Horn, D. M.; Carpenter, B. K.; McLafferty, F. W. *J. Am. Chem. Soc.* **1999**, *121*, 2857-2862.

(20) Kleinnijenhuis, A. J.; Mihalca, R.; Heeren, R. M. A.; Heck, A. J. R. *Int. J. Mass Spectrom.* **2006**, *253*, 217-224.

(21) Teesch, L. M.; Orlando, R. C.; Adams, J. *J. Am. Chem. Soc.* **1991**, *113*, 3668-3675.

(22) Kohtani, M.; Kinnear, B. S.; Jarrold, M. F. *J. Am. Chem. Soc.* **2000**, *122*, 12377-12378.

(23) Taraszka, J. A.; Li, J. W.; Clemmer, D. E. *J. Phys. Chem. B* **2000**, *104*, 4545-4551.

(24) Liu, D. F.; Seuthe, A. B.; Ehrler, O. T.; Zhang, X. H.; Wyttenbach, T.; Hsu, J. F.; Bowers, M. T. *J. Am. Chem. Soc.* **2005**, *127*, 2024-2025.

(25) Wyttenbach, T.; Bushnell, J. E.; Bowers, M. T. *J. Am. Chem. Soc.* **1998**, *120*, 5098-5103.

(26) Mihalca, R.; van der Burgt, Y. E. M.; Heck, A. J. R.; Heeren, R. M. A. *J. Mass Spectrom.* **2007**, *42*, 450-458.

(27) Williams, S. M.; Brodbelt, J. S. *J. Am. Soc. Mass Spectrom.* **2004**, *15*, 1039-1054.

(28) Lee, S. W.; Kim, H. S.; Beauchamp, J. L. *J. Am. Chem. Soc.* **1998**, *120*, 3188-3195.

(29) Kish, M. M.; Wesdemiotis, C. *Int. J. Mass Spectrom.* **2003**, *227*, 191-203.

(30) Nemirovskiy, O. V.; Gross, M. L. *J. Am. Soc. Mass Spectrom.* **1998**, *9*, 1285-1292.

(31) Tomlinson, M. J.; Scott, J. R.; Wilkins, C. L.; Wright, J. B.; White, W. E. *J. Mass Spectrom.* **1999**, *34*, 958-968.

(32) Gunawardena, H. P.; O'Hair, R. A. J.; McLuckey, S. A. *J. Proteome Res.* **2006**, *5*, 2087-2092.

(33) Grese, R. P.; Cerny, R. L.; Gross, M. L. *J. Am. Chem. Soc.* **1989**, *111*, 2835-2842.

(34) Hu, P. F.; Gross, M. L. *J. Am. Chem. Soc.* **1993**, *115*, 8821-8828.

(35) Lioe, H.; Duan, M.; O'Hair, R. A. J. *Rapid Commun. Mass Spectrom.* **2007**, *21*, 2727-2733.

(36) Wallis, T. P.; Pitt, J. J.; Gorman, J. J. *Protein Sci.* **2001**, *10*, 2251-2271.

(37) Luo, X. M.; Huang, W.; Mei, Y. H.; Zhou, S. Z.; Zhu, L. G. *Inorg. Chem.* **1999**, *38*, 1474-1480.

(38) Wei, H.; Luo, X. M.; Wu, Y. B.; Yao, Y.; Guo, Z. J.; Zhu, L. G. *J. Chem. Soc.-Dalton Trans.* **2000**, 4196-4200.

(39) Becke, A. D. *J. Chem. Phys.* **1993**, *98*, 5648-5652.

(40) Lee, C. T.; Yang, W. T.; Parr, R. G. *Phys. Rev. B* **1988**, *37*, 785-789.

(41) Harihara.Pc; Pople, J. A. *Chem. Phys. Lett.* **1972**, *16*, 217-&.

(42) Roepstorff, P.; Fohlman, J. *Biomed. Mass Spectrom.* **1984**, *11*, 601-601.

(43) Morris, H. R.; Pucci, P. *Biochem. Biophys. Res. Commun.* **1985**, *126*, 1122-1128.

(44) Sun, Y. P.; Smith, D. L. *Anal. Biochem.* **1988**, *172*, 130-138.

(45) Wysocki, V. H.; Tsaprailis, G.; Smith, L. L.; Breci, L. A. *J. Mass Spectrom.* **2000**, *35*, 1399-1406.

(46) Bilusich, D.; Brinkworth, C. S.; McAnoy, A. M.; Bowie, J. H. *Rapid Commun. Mass Spectrom.* **2003**, *17*, 2488-2494.

(47) Bowie, J. H.; Brinkworth, C. S.; Dua, S. *Mass Spectrom. Rev.* **2002**, *21*, 87-107.